

THE UNIVERSITY OF MICHIGAN
COLLEGE OF ENGINEERING
Department of Mechanical Engineering

Final Report

A STUDY OF HIGH-SPEED MILLING

Part I. The Role of Shock Waves and Vibrations

L. V. Colwell
L. J. Quackenbush

ORA Project 05038

under contract with:

J. E. RAMSEY
LA CANADA, CALIFORNIA

administered through:

OFFICE OF RESEARCH ADMINISTRATION ANN ARBOR

September 1962

engn

UMR 6676

TABLE OF CONTENTS

	Page
LIST OF TABLES	v
LIST OF FIGURES	vii
ABSTRACT	ix
I. INTRODUCTION	1
II. EARLY INDICATIONS	3
III. A SPECIFIC STUDY OF VIBRATIONS	11
A. The Cutting Tests	11
B. Summary of Cutting Data	19
IV. COROLLARY EVIDENCE	25
A. Impact Study	25
B. AMC Technical Report No. 60-7-635	25
V. SUMMARY	29
APPENDIX A. TYPES OF SOUND WAVES AND RESONANT VIBRATIONS	31
1. Internal vs. Mechanical Vibrations	32
2. Types of Waves	32
3. Calculated Frequencies	32
APPENDIX B. TABLES OF FREQUENCY DATA	39
APPENDIX C. ANALYSIS OF IMPACT CONDITIONS	45
REFERENCES	49

LIST OF TABLES

Table	Page
I Properties of Materials	13
II Wave Velocities	13
III Comparison of Experimental Results with Theoretical Predictions	22
IV Available Frequencies as Determined by Impact	26
V Striation Frequencies	27
VI Frequencies of Flexural Modes	34
VII Calculated Frequencies for Reflected Waves	35
VIII Frequencies of Shear Modes	36
IX Lengths of Quarter-Waves	40
X Frequencies of Chip Segments	41
XI Summary of Frequencies for Aluminum	42
XII Summary of Frequencies for Steel	43
XIII Summary of Frequencies for B-120-Titanium	44

LIST OF FIGURES

Figure		Page
1	Facemilling investigation of A-110 titanium: setup and records.	4
2	Effect of increasing overhang on the frequency of vibration in the shear mode.	5
3	Change in frequency of horizontal shock waves with increase in length of workpiece.	7
4	Experimental setup for monitoring vibrations and tangential cutting force components.	8
5	Cutting forces and tool accelerations for cuts of different length at constant cutting speed.	9
6	Chips obtained from experimental setup.	12
7	Setup for studying frequency of chip segmentation.	14
8	Oscilloscope traces for an aluminum test specimen.	15
9	Accelerometer signal for brass specimen.	16
10	Strain-gage signal for titanium specimen cut at different speeds.	17
11	Typical chip-segmentation characteristics.	20

ABSTRACT

It has been found that the brittle fracture sought by cutting metal at speeds beyond the velocity of a plastic wave front occurs as a natural phenomenon at much lower cutting speeds. It is shown that chip formation is influenced strongly by resonant vibrations not only of the tool and body motions of the workpiece but also by standing waves and reflected shock waves inside the workpiece and the cutting tool. In most cases the resulting frequencies of chip segmentation can be predicted from shear wave theory as was demonstrated during the ultra-high-speed machining investigation by Lockheed in 1960.

Practical consequences of this phenomenon include power consumption and chatter, with the notch sensitivity of metals involved as an important machining property. Feasibly, common chatter can at least be inhibited by superimposing higher-frequency vibrations in cutting those metals which have substantial notch or strain-rate sensitivity at cutting temperature. Power requirements can be substantially reduced when shear strain is decreased, as observed when ultrasonic vibrations are superimposed on metal cutting.

I. INTRODUCTION

Vibrations in metal cutting, particularly the common problem of chatter in machining operations have been the object of many research investigations. It is well known that chatter involves resonant vibrations of workpieces, cutting tools, work-holding devices, and other elements of the machine tool system. These resonant vibrations are characterized by such distinct body motions as bending of cutting tools and milling arbors and torsional vibrations of spindles.

The subject of this paper, however, is the role of sonic vibrations inside workpieces and cutting tools used in the cutting process. This paper is a byproduct of a study of high-speed milling wherein it became evident that resonant phenomena similar to chatter were occurring but without the familiar surface patterns and loss of size control. Subsequent investigations have indicated that these very-high-frequency, internal vibrations play an important role in the metal cutting process. They occur not only at high cutting speeds but over the entire range of commercial practice with regard to speed and size of cut. It appears feasible to use this natural phenomenon as an aid to better metal cutting. For example, it is evident that some of the beneficial effects of superimposed ultrasonic vibrations can be attributed to the reaction of metals to internal vibrations. Furthermore it would seem possible to prevent chatter by a similar approach.

II. EARLY INDICATIONS

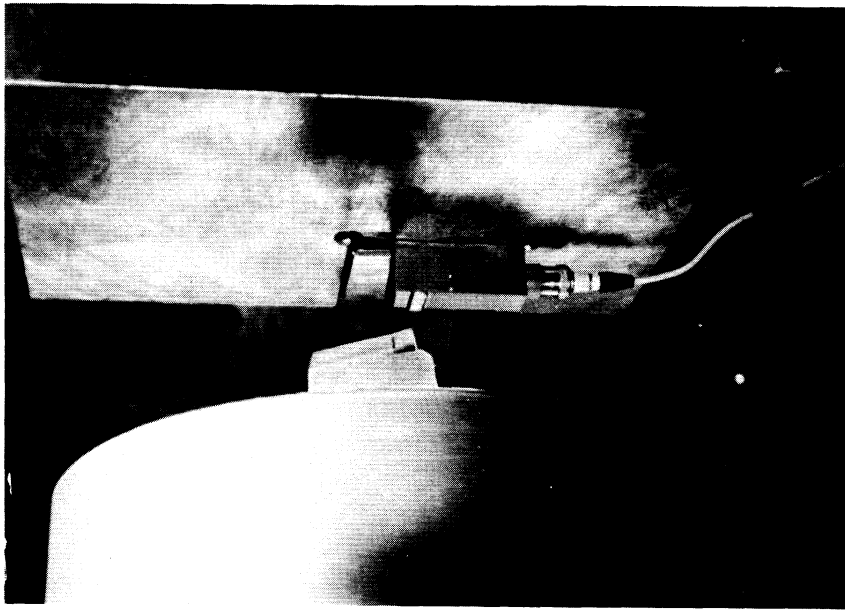
The initial evidence which led to the specific study upon which this paper is based came out of the investigation of ultra-high-speed machining by Lockheed (1) and a high-speed milling study performed at The University of Michigan. Measures were taken at the outset of the Michigan study to provide a high degree of rigidity in order to minimize vibration and to prevent common chatter. Chatter did not occur but there was evidence of high-frequency phenomena of a resonant nature in segmentation of the chips and in oscillographic records of cutting forces and vibrations. Figures 1 through 6 show information typical of that obtained in the initial study.

Figure 1 shows results from a facemilling investigation. The work specimen and single-tooth milling cutter are shown in Fig. 1(a) along with the accelerometer which produced the oscillographic records shown in Figs. 1, 2, and 3. The work specimen was fed radial to the rotation of the cutter spindle and parallel to the bright surface directly opposite the cutting tool.

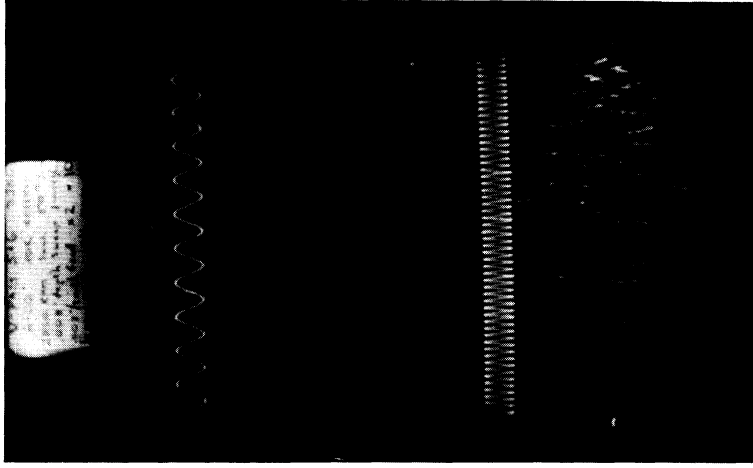
The oscilloscope records in Figs. 1(b) and 1(c) show the vibrations at cutting speeds of 3000 fpm and 4500 fpm respectively. It will be noted that the intensity of the vibrations is increased at the higher cutting speed, probably as a result of the higher impact velocities. The simple sine waves are 10-kc references. These indicate that the lower frequency is of the order of 4000 cps, whereas the higher frequencies are at least an order of magnitude greater.

Figure 2 shows that increasing overhang also increases the amplitude of vibrations. At the same time, the frequency of the vibrations appears to decrease, as would be expected from elementary theory on flexural and shear vibrations. The cutting time per chip was only 160 μ sec for the lower trace in all three cases, whereas that in the upper trace lasted 214 μ sec. The spindle speed was 1000 rpm so that the time per revolution was 0.066 sec.

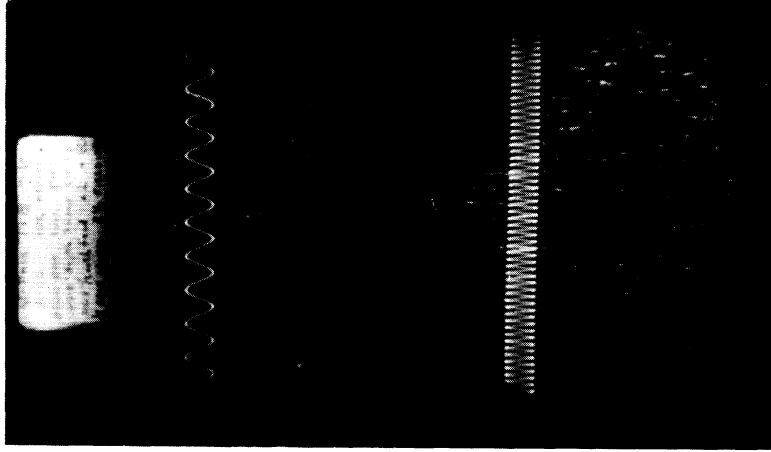
One can see that the vibrations lasted much longer than the cut but were completely damped out before the beginning of the next cut. The lower frequency which responded to the change in overhang appeared to be a flexural mode in the related direction although the frequency was lower than that predicted from the overhang as the length of a cantilever beam. However the method of clamping was such that the effective beam length must have been somewhat greater. An effective beam length of 1.4 in. would have accounted for the 7500-cps frequency, the lowest observed for the 15/16-in. overhang, as shown in Fig. 2(b). If the flexural vibration were to cause segmentation of the chip, then there would be no more than two such segments, since the period of the vibration is 130 μ sec compared with the cutting time of 160 to 214 μ sec. The chips showed many more



(a) Work specimen, single-tooth milling cutter, and accelerometer



(b) Accelerometer record (1-1/4-in. overhang; cutting speed: 3000 fpm)



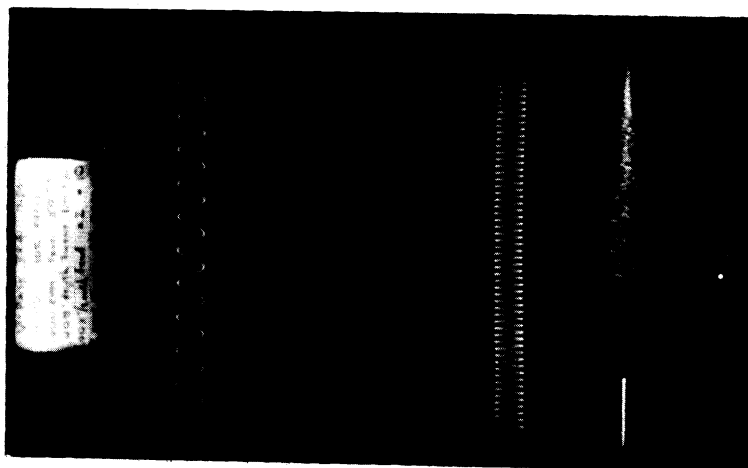
(c) Accelerometer record (1-1/4-in. overhang; cutting speed: 4500 fpm)

Fig. 1. Facemilling investigation of A-110 titanium: setup and records. Note that the higher impact at higher speed increases amplitude of lower-frequency vibrations; see Fig. 2 for lower speeds.

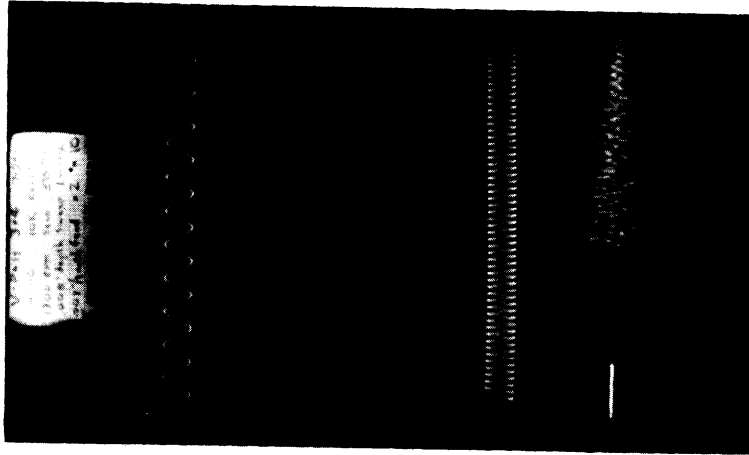
Sweep
Rate

0.1
msec/cm

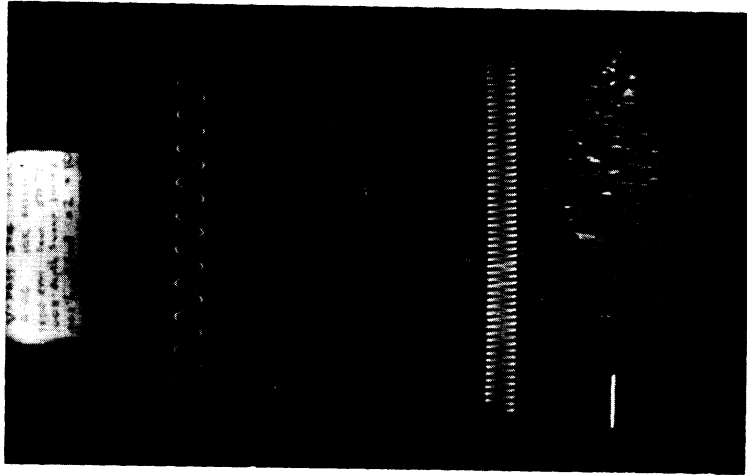
0.5
msec/cm



(a) 5/8-in. overhang



(b) 15/16-in. overhang



(c) 1-1/4-in. overhang

Fig. 2. Effect of increasing overhang on the frequency of vibration in the shear mode. A-110 titanium; vertical vibrations; time wave is 10 kc at both sweep rates; note increasing amplitude and decreasing frequency with increase in overhang; cutting speed = 1500 fpm; depth = .008 in.; feed = .008 ipt; A-110 titanium; vertical vibrations; time wave 10 kc at both sweep rates; see Fig. 1 for higher speeds.

than two segments, however, as is discussed in Section III. Thus doubt remained as to whether the vibrations were generated by segmentation.

Figure 3 shows similar information for a test series in which the length of the workpiece was varied while all the other conditions were held constant. In this series, the accelerometer was mounted on the rear of the workpiece directly opposite the cut; consequently the indications are referred to as horizontal vibrations. The frequencies were distinctly lower with the longer work specimens, suggesting that the vibrations were indeed resonant and dependent upon workpiece geometry and dimensions, and indicating that the vibrations were internal to the workpiece.

Another series of tests was carried out with the configuration illustrated in Fig. 4. The workpiece was rotated at a radius of 3 in. and interrupted cuts were made while the cutting tool was fed radially across the face of the workpiece. The load cell and accelerometer produced signals of the type shown in Fig. 5. This figure shows the forces and vibrations for cuts of different length made at constant cutting speed so that the duration of cut varied from 214 up to 588 μ sec.

The lower trace represents the cutting force and the motion of the cutting tool. It will be noted that the tool not only deflected under load but also vibrated during the cut. The flexural mode of vibration occurred at a frequency of about 6500 cps, which proved to be the resonant frequency of the tool as mounted. As in the case of the overhanging workpiece, the effective beam length was somewhat greater than the actual overhang.

The higher frequencies which are evident in both the force and accelerometer records appear to be the result of shock waves reflecting from the bottom of the tool. If such waves had traveled at the velocity of shear, the resultant frequency would have been of the order of 50 to 55 kc, depending upon the effects of the increased mass of the carbide tips. The accelerometer traces show a frequency of the order of 50 to 60 kcs.

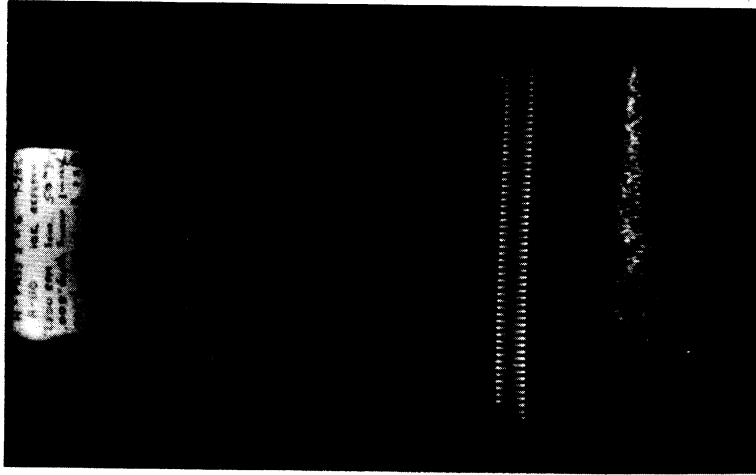
Examination of chips produced information of the type shown in Fig. 6. The chips shown in this figure were made with the setup shown in Fig. 4. The coarse segments along one edge of the chip correspond to a frequency of about 53,000 cps, but the major portion of chips show a segmentation frequency well in excess of 200,000 cps. Subsequent experience indicates that this frequency had to be a function of the thickness of the workpiece although it is not yet known whether the vibration waves are shear, dilatational, or surface waves.

Thus at the time of this first investigation there appeared to be some correlation between vibrations and the segmentation of chips. Furthermore the evidence was strong that the vibrations were resonant and were the cause rather than the result of segmentation. However, the geometry of both the workpieces and the tools was complex, which left some doubt as to whether the theoretical

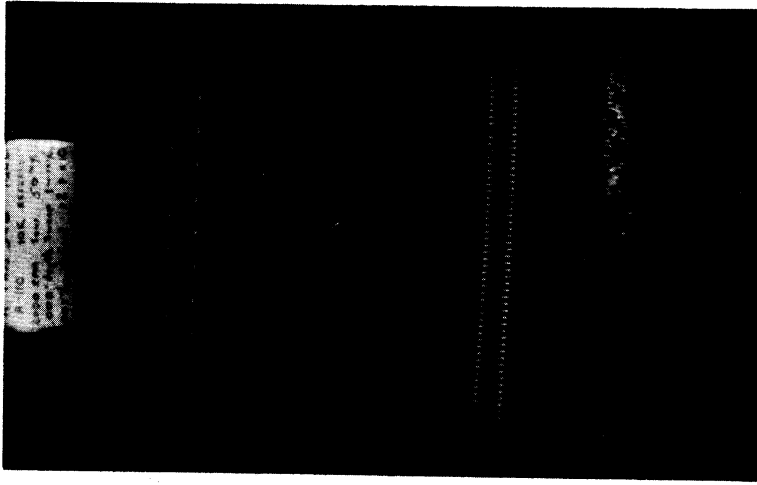
Sweep
Rate

0.1
msec/cm

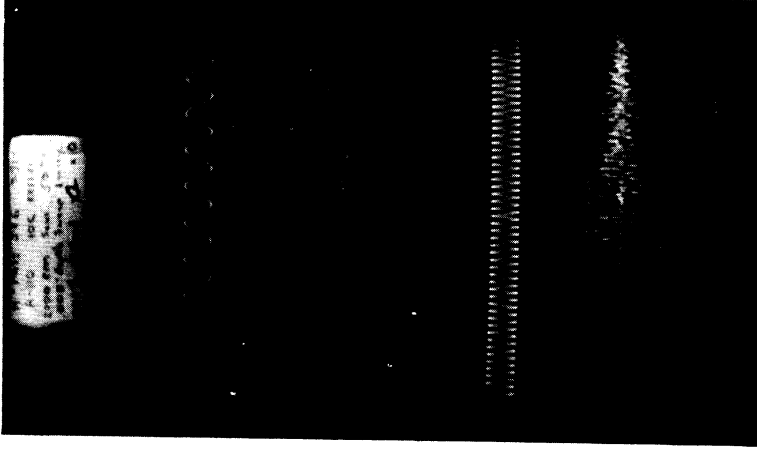
0.5
msec/cm



(a) Workpiece 2-1/8-in. long



(b) Workpiece 2-7/16-in. long



(c) Workpiece 2-3/4-in. long

Fig. 3. Change in frequency of horizontal shock waves with increases in length of workpiece. A-110 titanium; horizontal vibrations; time wave 10 kc at both sweep rates; cutting conditions same as in Fig. 2 except that cutting speed = 3000 fpm; workpiece overhang = 5/8 in.; accelerometer mounted on end of workpiece opposite of cut.

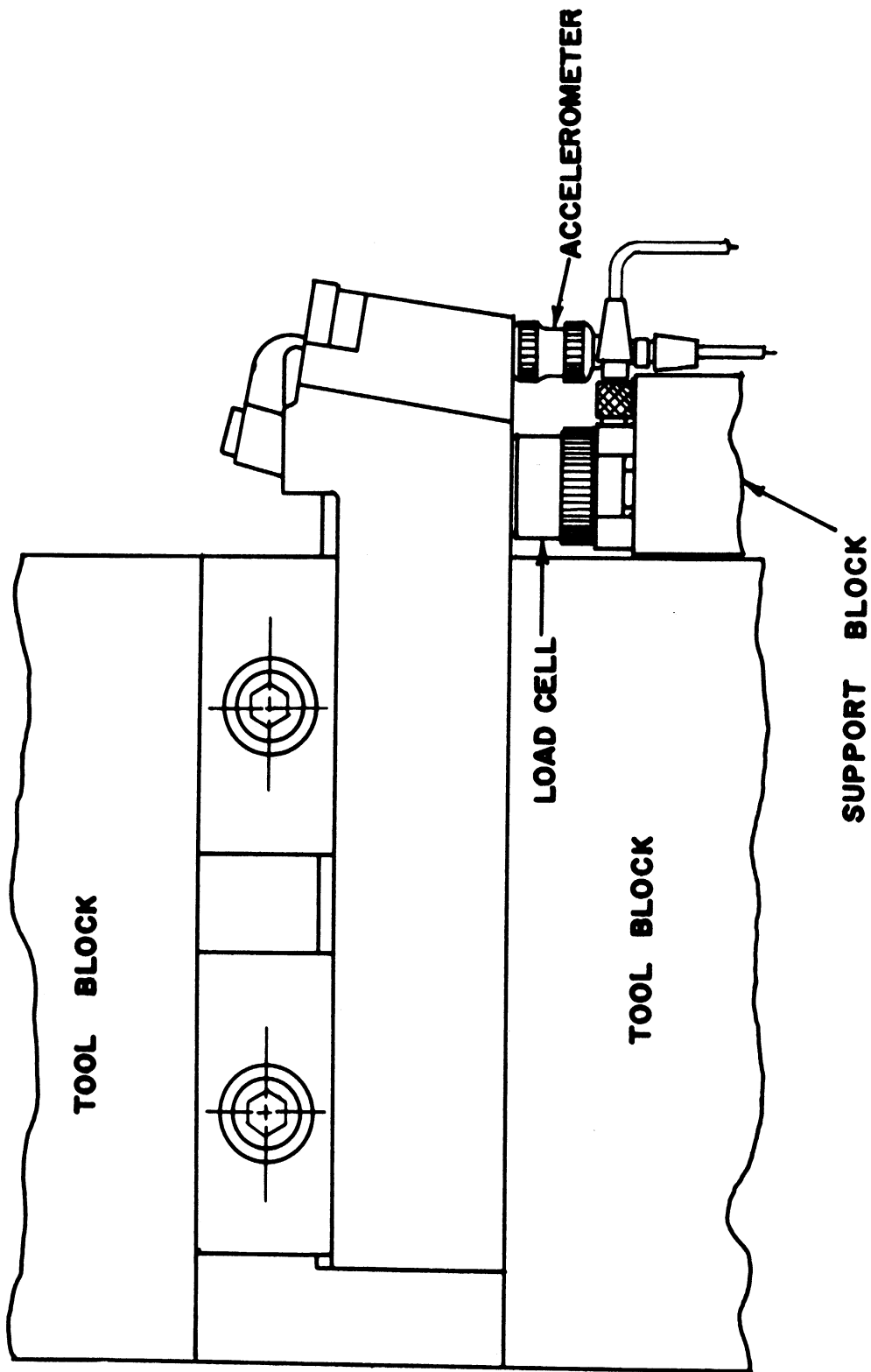
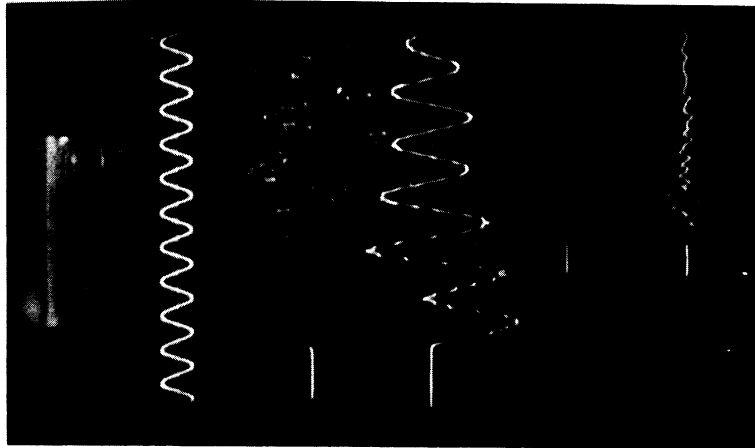


Fig. 4. Experimental setup for monitoring vibrations and tangential cutting-force component. Accelerometer and load-cell signals are fed to preamplifiers and then to a dual-beam oscilloscope, where they are recorded with a camera.

10 kc
Reference

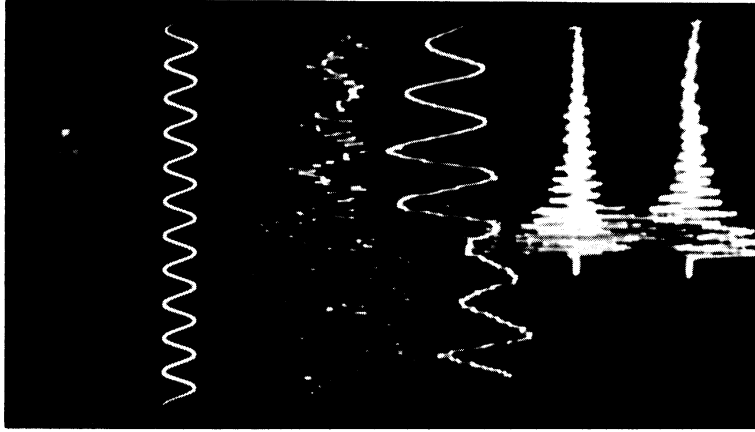
Acceleration

Force



Start ↗ ↘ Finish

(a) Duration of cut,
214 μ sec/chip
(Pass No. 4)



Time →

(b) Duration of cut,
535 μ sec/chip
(Pass No. 10)



Start ↗ ↘ Finish

(c) Duration of cut,
588 μ sec/chip
(Pass No. 11)

Fig. 5. Cutting forces and tool accelerations for cuts of different length at constant cutting speed. C-120 titanium; cutting speed = 1500 fpm; depth = .008 in.; feed = .008 ipt; sine wave at top is 10-kc time reference; cutting force and tool deflection is downward under load; force = 27.5 lb/cm of trace deflection.

analyses were sufficiently rigorous to constitute proof of resonance. Moreover many of the segmentation frequencies were very high and difficult to resolve accurately. Therefore a specific study was planned to overcome these difficulties and to resolve the remaining questions.

III. A SPECIFIC STUDY OF VIBRATIONS

This study consisted of three distinct parts. The first was a theoretical study wherein attempts were made to predict vibration frequencies by calculation. The second was made up of impact studies on actual work specimens to determine the resonant modes which could be excited by a single transient disturbance. The third consisted of laboratory machining tests in which vibrations of the workpiece were measured during cutting and chips were collected and analysed as to structure and frequency of segmentation.

A. THE CUTTING TESTS

Milling cuts were made with a single-tooth, rotating cutter and a workpiece that was stationary except for the feeding motion. A schematic diagram of the test arrangement is shown in Fig. 7. All of the work specimens were cylindrical rods of different lengths. A test section symmetrical to the centerline of the rod was machined on one end to provide for an orthogonal cut of constant width and length.

The work specimen was clamped rigidly between two steel blocks having cylindrical surfaces and a thin sheet of Teflon was placed between the blocks and the workpiece to minimize coupling with the rest of the system. Some specimens were equipped with strain gages on the periphery and an accelerometer on the end opposite the test section: others were equipped with an accelerometer only. Still others were equipped with neither strain gages nor an accelerometer as they were intended only for the accumulation of chips.

Tests were made at speeds ranging from 1575 to 6300 fpm and at feed rates or cut thicknesses of 0.002, 0.004, 0.006, 0.008 and 0.010 in. The workpieces were 1 in. in diameter and were 2, 2-1/2, 5, 10, 11, 11-1/2, 12 and 12-5/8 in. long. In addition, some tests were made with specimens 1/2 in. in diameter and 5 in. long. Physical properties and sound velocities of the work materials are listed in Tables I and II respectively.

Typical oscilloscope records are reproduced in Figs. 8,9, and 10. Figure 8 was obtained with an aluminum specimen. The traces in Fig. 8(a) are the result of a light tap with a hammer. They show a strong flexural mode which showed up during the cutting also. The frequency which was about 3600 cps, could have produced no more than three segments in a chip at the cutting conditions used in this case. The chips showed many more, however.

The traces in Fig. 8(b) show a much higher frequency superimposed on the bending mode. The lower trace is the difference between the strain-gage signal which was connected for bending and the accelerometer thus bucking out the bend-

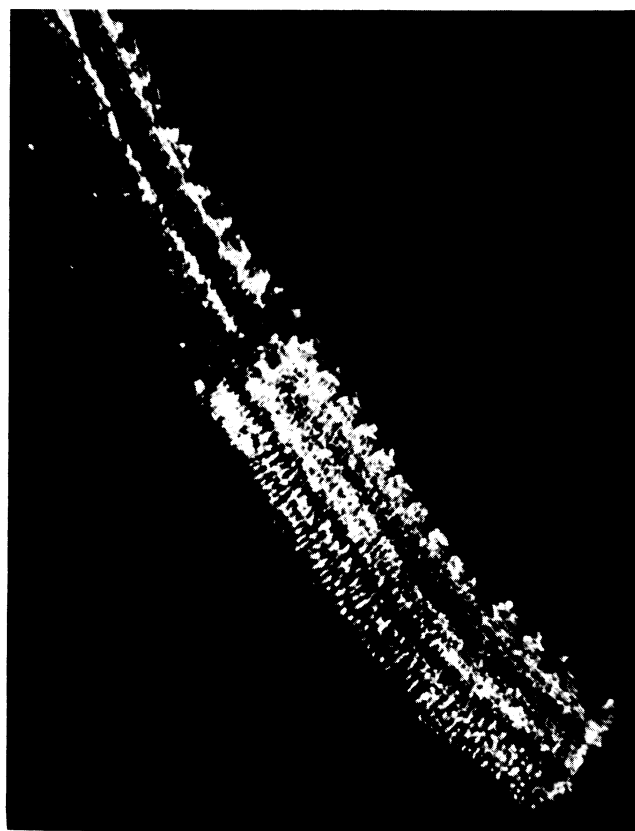
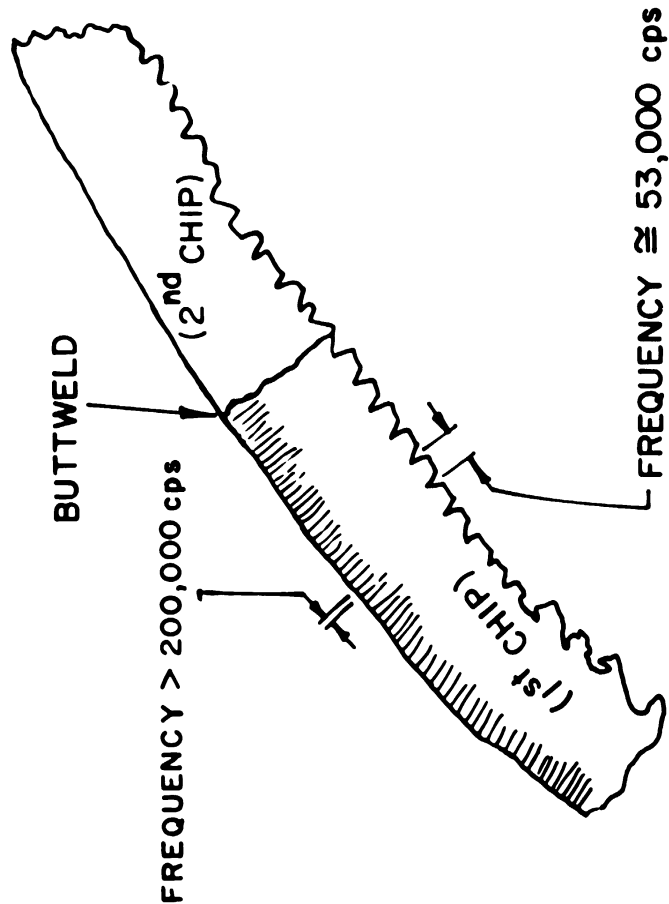


Fig. 6. Chips obtained from experimental setup. Pass No. 5; C-120 titanium; speed = 1500 fpm; feed = .002 ipt; depth = .008 in.; the 14 coarse segments occur at a frequency of about 53,000 cps, which corresponds to highest frequency shown by accelerometer.

TABLE I

PROPERTIES OF MATERIALS

Work Material	Modulus of Elasticity, psi			Density- ρ , lb/in. ³	Poisson's Ratio- σ
	Young's - E	Shear - G	Bulk - K		
Aluminum	10.2 x 10 ⁶	3.8 x 10 ⁶	11.0 x 10 ⁶	.101	.340
Brass	13.7 x 10 ⁶	5.3 x 10 ⁶	11.4 x 10 ⁶	.305	.295
Copper	17.2 x 10 ⁶	6.4 x 10 ⁶	18.0 x 10 ⁶	.324	.345
Steel (Carbon)	29.8 x 10 ⁶	11.5 x 10 ⁶	23.4 x 10 ⁶	.283	.287
Steel (Stainless)	29.7 x 10 ⁶	11.4 x 10 ⁶	25.6 x 10 ⁶	.320	.307
Titanium (A110)	16.0 x 10 ⁶	6.0 x 10 ⁶	16.0 x 10 ⁶	.161	.332
Titanium (B120)	14.2 x 10 ⁶	5.45 x 10 ⁶	12.1 x 10 ⁶	.175	.304
Titanium (C120)	15.8 x 10 ⁶	6.0 x 10 ⁶	15.7 x 10 ⁶	.160	.318

TABLE II

WAVE VELOCITIES
(x10⁵ ips)

Work Material	Type of Wave		
	Bulk	Longitudinal	Shear
Aluminum	2.49	2.00	1.21
Brass	1.58	1.32	.818
Copper	1.80	1.44	.875
Steel (Carbon)	2.33	2.02	1.25
Steel (Stainless)	2.58	1.89	1.17
Titanium (A110)	2.40	1.96	1.20
Titanium (B120)	2.41	1.77	1.10
Titanium (C120)	2.34	1.96	1.20

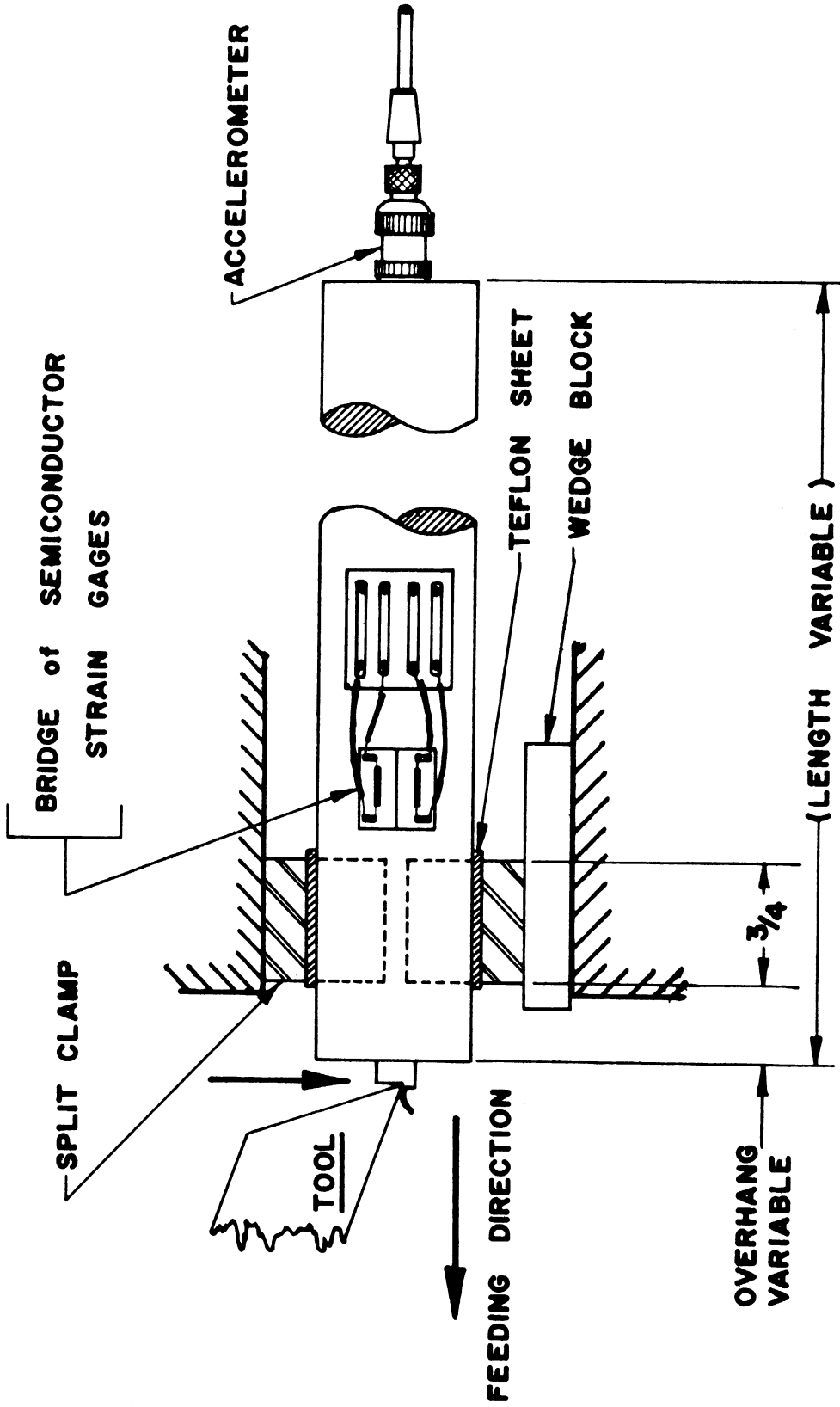
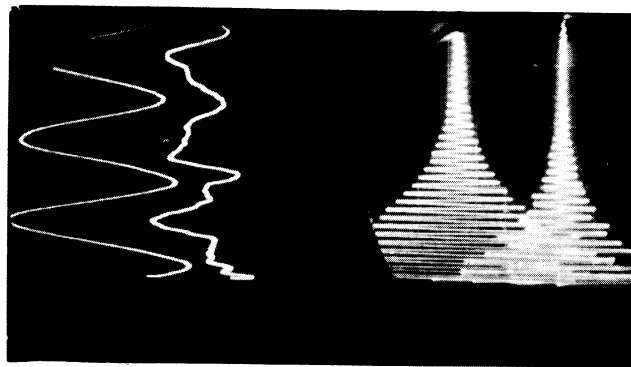
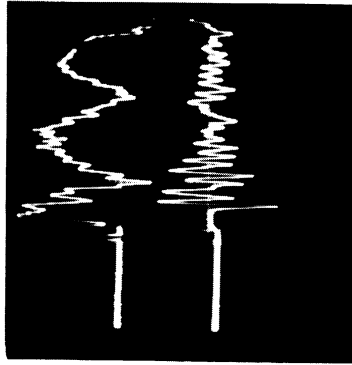


Fig. 7. Setup for studying frequency of chip segmentation. A thin sheet of Teflon is placed between the work specimen and the split clamping block to minimize transmission of vibrations at this point; a variable-speed transmission provides controlled feed rate to a lead screw through an electromagnetic clutch and brake assembly.

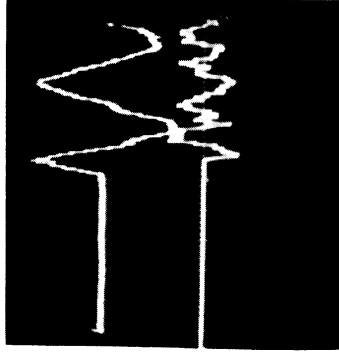


Sweep Rate
 100 $\mu\text{sec}/\text{cm}$
 1000 $\mu\text{sec}/\text{cm}$



(b)

Sweep rate = 100 $\mu\text{sec}/\text{cm}$
 Cutting time = 634 $\mu\text{sec}/\text{chip}$
 Cutting speed = 1575 fpm

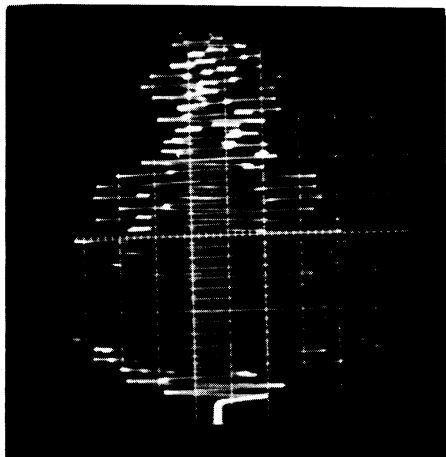


(c)

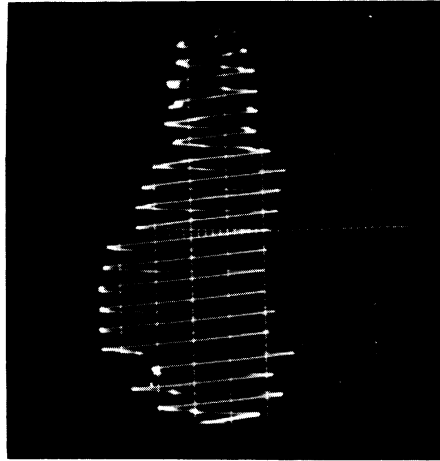
= 100 $\mu\text{sec}/\text{cm}$
 = 634 $\mu\text{sec}/\text{chip}$
 = 1575 fpm

(a) Vibrations caused by hammer blow

Fig. 8. Oscilloscope traces for an aluminum test specimen. The upper trace is the strain-gage signal; the lower trace was produced by the accelerometer; length of cut = .200 in.; width of cut = .060 in. feed = .008 ipt; work specimen was 1 in. in diameter and 12.64 in. long.

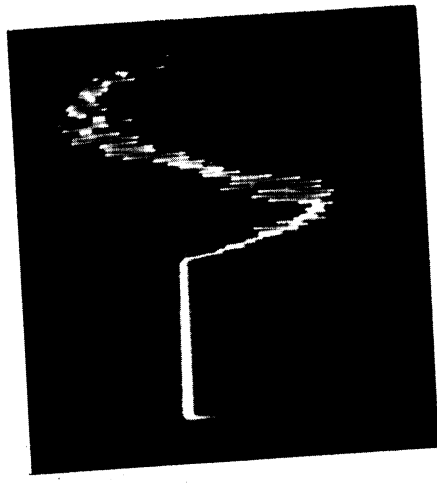


(a) 100 $\mu\text{sec}/\text{cm}$



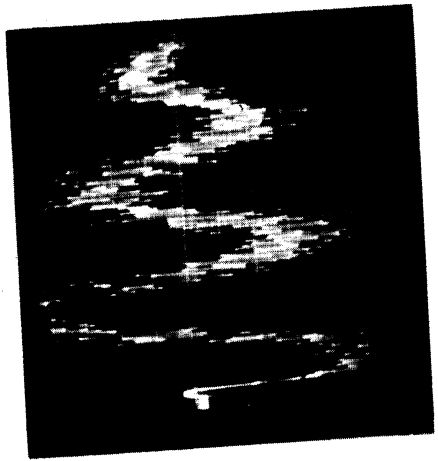
(b) 50 $\mu\text{sec}/\text{cm}$

Fig 9. Accelerometer signal for brass specimen. Cutting time = 317 $\mu\text{sec}/\text{chip}$; cutting speed = 3150 fpm; feed rate = .010 ipt; test surface was .060 in. wide and .200 in. long; test bar was 1 in. in diameter and 6-7/8 in. long; note relative absence of flexural mode.



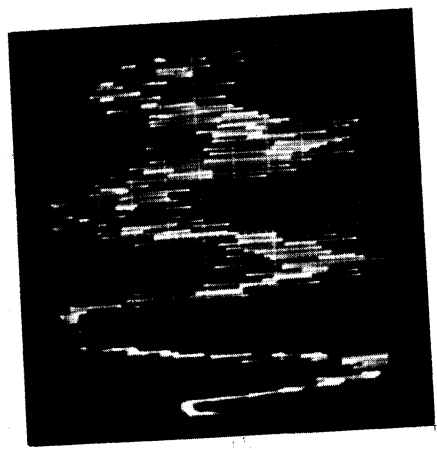
(c)

= 50 μ sec/cm
 = 1575 fpm
 = 3170 μ sec/chip



(b)

= 100 μ sec/cm
 = 3150 fpm
 = 1585 μ sec/chip



(a)

= 100 μ sec/cm
 = 1575 fpm
 = 3170 μ sec/chip

Sweep rate
 Cutting speed
 Cutting time

Fig. 10. Strain-gage signal for titanium specimen cut at different speeds. Feed rate = .005 ipt; test surface was 1.000 in. long and .100 in. wide; test bar was 12-1/2 in. long and 1.000 in. in diameter; note tendency for higher speed to increase the high frequencies superimposed on the fluxural mode.

ing signal from the accelerometer. The result shows a strong mode just above 30 kc, which was the dominant frequency in the chips. The traces in Fig. 8(c) were independent of each other. It will be noted that the initial signals from the strain gages and the accelerometer occurred about 50 μ sec apart. This indicates that the initial shock wave was dilatational instead of shear since the accelerometer was 10-1/2 in. from the strain gages.

The accelerometer traces in Fig. 9 illustrate two significant features of the problem. The first is the work material. In this case the material is leaded brass, which is well known as a free-cutting material because of the ease with which the chips can be broken up. Both traces show the dominance of a single frequency during the cut, which lasted 317 μ sec. This characteristic proved to be somewhat unique to such metals as brass, magnesium, and titanium, and might properly be called notch sensitivity or brittleness. Brittleness is accompanied by abruptness and sudden fracture; this in turn produces a sudden change in cutting force which can excite or sustain a forced vibration.

Theoretically, all harmonics of the vibration result from a single disturbance of a system. In practice, however, all harmonics which produce particle velocities sufficient to cause brittle fracture could produce chip segmentation. Thus it is natural for a standing wave to develop at one frequency since the nodal points of all lower harmonics coincide in point of time. The 36-kc frequency shown in Fig. 9 corresponds to a shear wave involving three full wavelengths longitudinal to the brass rod. The 6-7/8-in. wavelength would cause the bar to resonate at the same frequencies as a bar of aluminum 10 in. long.

The second significant feature revealed in Fig. 9 is the finite but short time required for the single frequency to become dominant and to establish a standing wave. It will be noted that only five or six cycles or about .0001 sec were required to achieve this condition. This is in contrast to the time required for aluminum and steel, which was long enough to allow frequencies of chip segmentation to be observed. The short time requirement for brass indicates that both transient shock and reflected waves can be present to a significant degree in materials which are more ductile or exhibit stronger damping properties.

Figure 10 illustrates another important factor related to cutting speed. It will be noted that the higher speed of 3150 fpm shown in Fig. 10(b) is accompanied by a distinctly higher frequency than that shown in Fig. 10(a) as accompanying a speed of 1575 fpm. This is typical of all the metals studied in this investigation. It would appear that the higher impact velocities associated with the higher speeds can force higher frequencies because of the larger stress gradients which make it possible for low amplitude vibrations to be effective.

A similar trend was noted in relation to the thickness of cuts. Thinner cuts generally show a higher frequency of segmentation for the same cutting speed. For example a cut 0.010 in. thick might give a segmentation frequency

of 24 kc at a speed of 3000 fpm and a cut 0.008 in. thick might give a segmentation frequency of 36 kc at the same speed. On the other hand both thicknesses might give a frequency of 24 kc at a speed of 2500 fpm. This is further evidence of the resonant origin of chip segmentation.

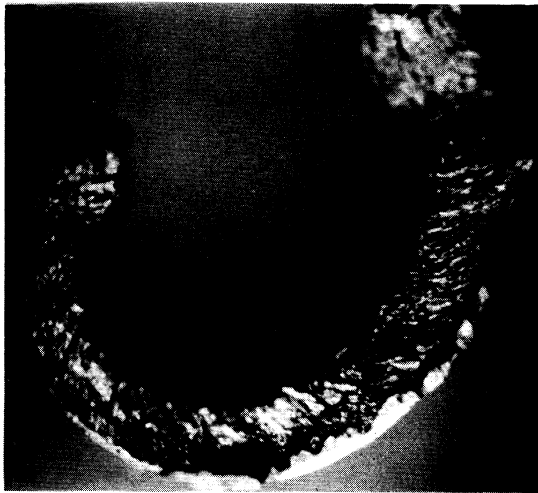
Typical chip-segmentation characteristics are illustrated in Fig. 11. The three chips represent three distinct conditions likely to be encountered. The 1018 Steel chip in Fig. 11(a) shows no measurable segmentation and might be called absolutely continuous. This condition does not hold at lower speeds, however, chips of the same material looked more like the one for aluminum as shown in Fig. 11(b). Similarly 1042 Steel showed strong segmentation at 3150 fpm but not as strong as at some of the lower speeds. It could be that the temperature in the shear zone was sufficiently high at the cutting speed of 3150 fpm to reduce brittleness or notch sensitivity to a level where sudden shear could no longer occur. Segmentation can be expected to reappear at yet higher speeds, however, as was observed in some of the exploratory tests.

The aluminum chip is representative of a condition which occurs frequently but not predominately in the cutting of relatively ductile metals like aluminum and steel. The chip is characterized by relatively coarse segments but in one region, near the middle, it is segmented less severely but at a frequency about three times as great. This condition is called a "mixed frequency" and can be attributed to reflections and transients since it never occurred at the beginning of a cut. These transient, high-frequency zones represent an incipient stage in the transition to a still higher frequency. A moderate increase in speed or decrease in thickness of cut causes the chip to display only the higher frequency.

The chip in Fig. 11(c) is typical of the most uniform segmentation; it is not from an orthogonal cut but was formed in a conventional facing out with a sharp-nosed tool. The coarser segments occurred at a frequency of 169,000 cps, which was found to be the resonant fundamental of the thickness of the work specimen. It is interesting to note that the thinner edge of the same chip shows still higher frequencies that are integral multiples of the lowest frequencies. These appear to be harmonics of the thickness of the specimen, although such high frequencies could also be resonant modes of the carbide tool insert.

B. SUMMARY OF CUTTING DATA

It was both difficult and expensive to try to substantiate all cutting data with oscillographic records. Therefore tests of this type were carried out only to confirm a positive correlation between chip segmentation and internal vibration frequencies. The major mass of data consists of counts of chip segments converted to frequency in cycles per second.



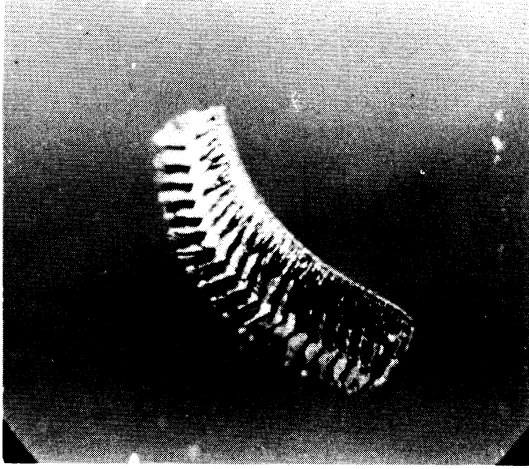
(a) 1018 Steel

Cutting speed = 3150 fpm
 Cutting time = 317 μ sec/chip
 Segmentation = None
 Frequency



(b) Aluminum

= 6300 fpm
 = 158 μ sec/chip
 = 94,800 cps



(c) Nivco-10

= 4500 fpm
 = 124 μ sec/chip
 = 169,000 cps

Fig. 11. Typical chip-segmentation characteristics. Different degrees and types of segmentation are produced by different combinations of cutting conditions and work materials; note absence of discrete segments in 1018 steel; note also the higher frequency in the thinned portions of the chip of Nivco-10.

The data on segmentation frequency for the specimens 2 1/2, 5, and 10 in. long are summarized in Table III. Data for aluminum, 1018 steel, 1040 steel, high carbon drill rod and titanium are lumped together since the shear velocities for all these materials are very close to each other. (Detailed summaries of the measured frequencies are given in the five Tables in Appendix B.) Table III contains both measured and predicted frequencies. It will be noted that the averages of measured values lie very close to predictions based on shear modes. In most cases the total scatter represented by the full range of all values counted into the averages is insufficient to bridge the gap to the next higher frequency.

The scatter can be attributed to several factors. Most important is the difficulty involved in making accurate counts of high frequencies with low-resolution microscopes. Second is the fact that the actual counts in chips showing mixed frequencies were added into the averages. In short cups the initial shock wave traveling at a speed higher than shear could add one extra segment as it reflected from the rear end of the rod. Similarly, flexural modes could add a few extra segments in chips from the cuts 1 in. long. Finally, there may possibly be sufficient damping in the more ductile materials to cause some lowering of the resonant frequencies.

Probably the most convincing evidence of the resonant nature of chip segmentation is the fact that the same frequency can persist over wide ranges of cutting speed and thickness of cut. For example, the average frequency of 37,140 cps occurred in 29 different tests involving combinations of three different speeds and four different thicknesses of cut. The speeds ranged from 4725 to 1575 fpm and the cut thicknesses from 0.002 to 0.010 in. Counts from more than a hundred chips are included in the average for a total scatter of only 18%.

Frequencies were calculated for all types of vibratory modes except for torsion. The equations used and tables of the frequencies are included in Appendix A. Comparison of the measured with the calculated frequencies shows the dominance of shear in the lower-frequency range. It may also dominate in the higher range but the close proximity of the frequencies of shear and longitudinal modes as the wavelength approaches the bar diameter makes it difficult to distinguish between them.

Further analysis of the frequencies in relation to the total length of the bar showed a strong preference for the frequencies to jump by gradients corresponding to the addition of one-half wavelength in the mode of vibration. The one exception was the occurrence of the 12.2-kc frequency specimens 2-1/2 in. long. This jump in frequency would seem to indicate that the entire length of the specimen consisted of only one quarter-wave. It could be argued that such an unstable state could be sustained as forced vibration. On the other hand it could be argued that only every second cycle of a half-wave mode is effective because the forward motion of the tool has not been able to build up sufficient

TABLE III

COMPARISON OF EXPERIMENTAL RESULTS WITH THEORETICAL PREDICTIONS

Frequency, cps		No. of Tests	No. of Different Speeds and of Feeds at Each Frequency		Total Scatter of Measured Frequencies		Frequency Gradients, cps	
Predicted	Measured		Speeds	Feeds	%	cps	Theoretical	Measured
12,200	12,820	18	1	2	31	4,000	--	--
	12,780	17**	1	2	24	3,100	--	--
18,300	17,800	3	1	1	9	1,600	6,100	5,000
24,400	24,200	3	2	2	13	2,900	6,100	6,400
36,600	37,140	29	3	4	18	6,600	12,200	12,960
48,800	49,100	9	3	2	13	6,500	12,200	11,960
61,000	63,000	3	1	2	0	--	12,200	13,900
97,600	98,800	9	1	2	15	15,000	36,600	35,800
100,000*								
122,000	124,700	4	2	1	14	17,000	24,400	22,700
200,000*	193,600	9	1	1	10	20,000	--	--

stress for the alternate cycle to trigger off a segment. These among other questions require further study with more advanced instrumentation.

IV. COROLLARY EVIDENCE

Two other sources of information were analysed because of their close relationship to the problem. One source is derived from an impact study which yielded some information on the frequency of transient vibrations which could nucleate the forced frequencies observed during cutting. The other source is the AMC Technical Report "Ultra High Speed Machining"¹, which reported similar results in 1960.

A. IMPACT STUDY

Tests were carried out wherein a 1/4-in. steel ball was dropped from a height of 9 in., making contact in various ways with an aluminum rod 1 in. in diameter and 11-7/8 in. long. The rod had semiconductor strain gages and an accelerometer mounted on it. The resultant inelastic impact produced transient vibrations which were displayed and photographed on an oscilloscope. The photographs were analysed by three persons and the results are summarized in Table IV along with possible frequencies derived from calculations. An analysis of the impact conditions is given in Appendix C.

The results show a strong correlation between the observed frequencies and those calculated for shear waves. There is no doubt that flexural modes were excited by lateral impact but it was evident that they dispersed into shear waves within a cycle or two. There is some doubt whether the highest frequency was a shear mode since the accelerometer gave strong signals at 100 kc when placed transverse to the direction of impact for both radial and longitudinal impact directions. On the whole, the impact investigation on one of the actual machining specimens indicated a strong probability that the forced vibrations in machining would be shear modes. This probability is supported also by the fact that flexural waves will disperse into shear and that the area of the shear plane in the cut is too small in relation to the diameter of the rod to initiate a plane longitudinal wave.

B. AMC TECHNICAL REPORT NO. 60-7-635¹

The final report "Ultra High Speed Machining," issued in June 1960 by the United States Air Materiel Command, contains experimental data which parallel the results of this paper. Table 19, p. 131, of the AMC Report lists the frequencies of striations which occurred on the machined surfaces of the projectile-type workpieces used as test specimens. The striations were straight lines perpendicular to the cutting direction and their spacing was regular enough to be reported as having occurred at a particular average frequency.

TABLE IV
AVAILABLE FREQUENCIES AS DETERMINED BY IMPACT
(kcs)

Flexural	Predicted Frequencies		Measured Frequencies	No. of Readings	Scatter	
	Shear Waves				%	kc
---	102.5		98.50	15	20	20.0
31.20	30.9		31.50	25	21	6.7
23.60	25.60		25.38	10	9	2.3
---	20.50		20.36	5	14	2.9
16.70	15.40		15.70	7	8	1.2
11.25	10.30		10.77	4	31	3.3
3.48 or 6.65	5.14		5.07	8	17	0.85

TABLE V

STRIATION FREQUENCIES*

(kcs)

		Active Length = $n\lambda/4$							
		n=1	n=2	n=3	n=4	n=5	n=6	n=7	n=8
Measured Data	No. of Readings	--	9	11	11**	5	9**	3	2**
	Range, kc	--	2.5	2.5	5.5	4.6	4.2	3.0	8.0
	Average Frequency	--	12.33	17.03	22.54	25.90	31.10	36.37	44.0
Predictions	Based on 5-1/2-in. Active Length	5.54	11.10	16.6	22.2	27.60	33.30	38.80	44.4
	Based on 6-in. Active Length	5.07	10.15	15.22	20.30	25.37	30.5	35.6	40.67

*Frequencies taken from Table 19 of Report No. LR 14021, Lockheed Aircraft Corporation; data are included for both steel and titanium since the shear velocities of both materials are nearly the same.

**Readings for projectiles 3-in. and 6-in. long are included; the 3-in. projectiles would have only half as many quarter-waves as the 6-in. projectiles.

These frequencies have been averaged and are summarized in Table V along with predicted frequencies based in longitudinal shear waves. All of the projectiles included in this summary had 1/2-in. diameter holes drilled on the centerline from the front to within 1/2-in. of the base. Therefore frequency calculations were made for active lengths of 6 in. and 5-1/2 in. since there is some doubt whether the base of the projectile would participate in a standing wave except as a boundary condition. The correlation seems rather good despite the fact that data for 3 in. projectiles was included with those for the 6 in. projectiles. The frequencies for the 3 in. projectiles were somewhat higher than the averages of the categories in which they were included. This might be expected because the length of the quarter-wave based on an active length of 2-1/2-in. would be somewhat shorter than that for 6 in. projectiles.

The Lockheed investigators attributed the striations to traveling shear waves and tried to explain frequency differences on the basis of the Doppler effect, in which case the frequency would approach infinity near the end of the cut and would be superimposed on the constant low frequency of the wave which reflects back and forth between the ends of the projectile. Traveling waves undoubtedly occurred to a significant degree at the very high impact speeds in the Lockheed tests but this could not explain the high frequencies encountered in the current investigation. Therefore it must be concluded that standing waves play a dominant role in chip segmentation and the associated formation of striations on the workpiece.

Other information produced by the Lockheed investigation which parallels the results of this paper involves the measurement of chip velocities (See Reference 1, Table 15, p. 104). In all but one case these chip velocities were higher than the cutting speed. It is now known that this seeming paradox results from abnormal segmentation wherein the stress gradient of the vibration is so large that considerable relative movement takes place between adjacent segments. It is accompanied by a positive rotation of the shear plane after the sudden shear fracture has taken place (See Reference 1, Table 24, p. 186). This lengthens the chip in much the same way that a deck of cards can be spread to a considerable length with the cards still overlapping each other. Consequently, the higher the frequency of segmentation, the greater this lengthening can become before the chip is broken up into discrete segments.

V. SUMMARY

The phenomena discussed here do not constitute a new theory of chatter but they do indicate that the role of vibrations in metal cutting is greater than it was previously thought to be. These phenomena involve internal vibrations or resonant noise, whereas chatter vibrations involve body motions. Both depend upon the same fundamental laws but chatter can be called a problem in mechanical vibrations whereas the other is more acoustical in nature.

It is believed that this discovery not only provides further explanation of the metal cutting process but also suggests benefits which might be derived from further research.

Dr. Von Karman suggested some years ago that if metal were cut at a speed in excess of the velocity of plastic wave propagation, the result would be brittle fracture accompanied by a reduction in energy requirements. This theory provided the basis for the Lockheed project on ultra-high-speed machining, and the achievements of that project are already significant in current metal cutting practice. Sound waves provide the real cutting speed and the velocity which we now call cutting speed is in reality just another feeding motion.

The reduction of energy requirements predicted by Dr. Von Karman has already been observed and is the object of a continuing study. It appears reasonably certain that at least part of the reduced energy requirements observed when ultrasonic vibrations are superimposed on machining operations can be attributed to this phenomenon.

Another useful exploitation of this property would be the prevention of chatter by superimposing a vibration of an amplitude sufficient to cause brittle segmentation and of a frequency high and dynamically remote from the chatter frequencies of the system.

APPENDIX A

TYPES OF SOUND WAVES AND RESONANT VIBRATIONS

Confusion and misinterpretation are likely to result from a discussion of vibrations and sound unless the words used to describe various phenomena are clearly understood. For this reason, the tables and equations presented in this appendix are accompanied by a definition and explanation of the nomenclature used.

1. INTERNAL VS. MECHANICAL VIBRATIONS

In the preceding report internal vibrations are distinguished from external or mechanical vibrations. It is difficult to provide a rigorous definition which separate the two since the differential equations or equations of state are similar in both areas.

Mechanical vibrations are simple compared with internal vibrations and involve relationships which can be represented by discrete masses, springs, and friction elements. Vibratory amplitudes are relatively large, frequencies are relatively low, and the concept of resonance is always involved. By contrast, internal vibration invokes the concept of waves and wave fronts which always travel through the medium with the velocity of sound. This is the principle reason for referring to such phenomena as "internal". The wave concept overlaps the area of mechanical vibrations in the vibrations of strings and the lateral vibrations of beams.

2. TYPES OF WAVES

There are several bases for classifying the different types of waves in solids. One important classification is that of traveling waves and standing waves. A traveling wave is like the wave set up in a rope or ship when one end is snapped suddenly, standing waves are like the vibrations of a violin string and are produced by the movement of two traveling waves in opposite directions at the same velocity. Thus the existence of standing waves is the condition of resonance in internal vibrations. It is important to remember that internal standing waves are two traveling waves, since this is what links the frequencies of standing waves and reflected waves which are identical.

3. CALCULATED FREQUENCIES

Tables VI, VII and VIII contain the frequencies calculated for interpretation of the results of this study. All of the frequencies are resonant frequencies and therefore involve standing waves.

Table VI contains the frequencies of bending or flexural modes. This is

classified as an external or mechanical vibration and the frequency equation, derived from simple bending theory is:

$$\omega_n = \frac{nk_2}{l} \sqrt{\frac{E}{\rho}} \quad (1)$$

where

- E = Young's Modulus (psi)
- ρ = density (Mass per unit volume)
- ω_n = natural frequency in radians per second
- k = radius of gyration in inches (R/2 for a circular section)
- l = length of inches
- n = coefficient depending on end and support conditions

Values of the coefficient (n) can be found in handbooks.

The concept of wave velocity is significant in bending for the treatment of transients which when combined with reflections could grow into standing waves. An equation for the velocity of such waves is:

$$(C_f)^2 = k\omega C_l \quad (2)$$

where

- C_f = velocity of flexural waves
- k = radius of gyration
- ω = frequency in radius per second
- C_l = velocity of plane waves in solids = $\sqrt{\frac{E}{\rho}}$

Equation (2) shows that the wave velocity increases with the sharpness or frequency of the transient. Consequently the frequencies of standing waves from Eq. (1) become meaningless as the wave velocity approaches the velocity of sound in shear. This is also an indication of why a transient flexural vibration will change over to or disperse into a shear wave.

Table VII contains the frequencies calculated for reflected waves which might occur as a result of the particular geometry and dimensions of the machining specimens and their method of support, as illustrated in Fig. 7. They are also the frequencies of the standing waves associated with the reflections, and were calculated from the relationships expressed in Eqs. (3), (4), and (5):

TABLE VI

FREQUENCIES OF FLEXURAL MODES*
(kcs)

Mode	Length of Free-Free Beam, in.				
	12	11	10	5	2-1/2
Fundamental	1.24	1.48	1.78	7.12	28.48
1st Harmonic**	3.40	4.05	4.90	19.60	78.40
2nd Harmonic	6.65	7.92	9.60	38.40	153.60
3rd Harmonic	11.00	13.10	15.90	63.50	***
4th Harmonic	16.35	19.50	23.60	94.80	***
5th Harmonic	23.00	27.40	33.20	133.50	***

*Frequencies calculated for aluminum free-free rods 1 in. in diameter. Frequencies for steel would be slightly higher and those for titanium about 12% lower.

**The first harmonic of a cantilever corresponds to the frequency of the fundamental of a free-free beam; the second harmonic corresponds to the first harmonic of the free-free beam; and so forth. The fundamental frequency of a cantilever is 17% of the fundamental frequency of a free-free beam.

***Higher harmonics are meaningless because the theoretical velocity of shear waves at a frequency of 46 kcs.

TABLE VII

CALCULATED FREQUENCIES FOR REFLECTED WAVES*

Work Material	Dia., in.	Total Length, a+b (in.)	Overhang, a (in.)	Longitudinal [†]			Shear ^{††}				
				a**	b**	a+b***	d	a	b	a+b	
Aluminum	1	10	7/8	57	5.5	10	100	34.8	3.35	6.1	61
	1	10	1-7/8	26.6	6.1	10	100	16.2	3.75	6.1	61
	1	5	7/8	57	11.6	20	100	34.8	7.05	12.2	61
	1	5	1-7/8	26.6	16.0	20	100	16.2	9.75	12.2	61
	1	2-1/2	7/8	57.0	30.1	40	100	34.8	18.8	24.4	61
	1/2	5	7/8	57.0	11.6	20	200	34.8	7.05	12.2	122
	1/2	5	1-7/8	26.6	16.0	20	200	16.2	9.75	12.2	122

*See diagram below

**Quarter-wave mode

***Half-wave mode

†Based on a plane-wave velocity of 200,000 ips

††Based on shear-wave velocity of 122,000 ips

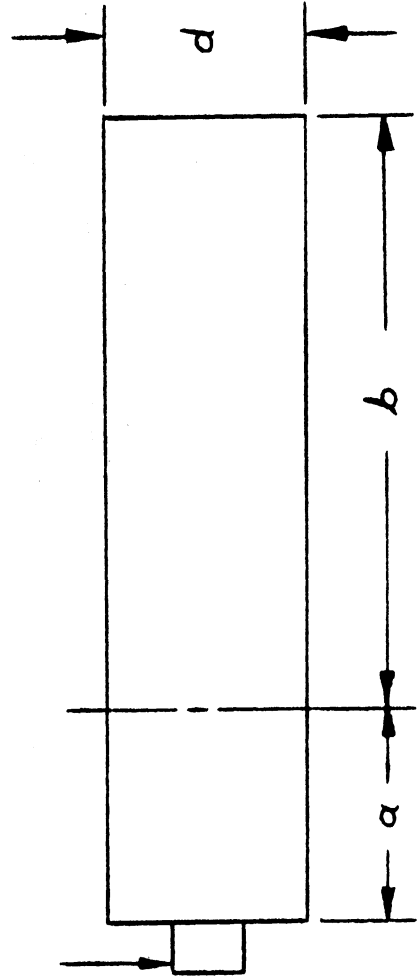
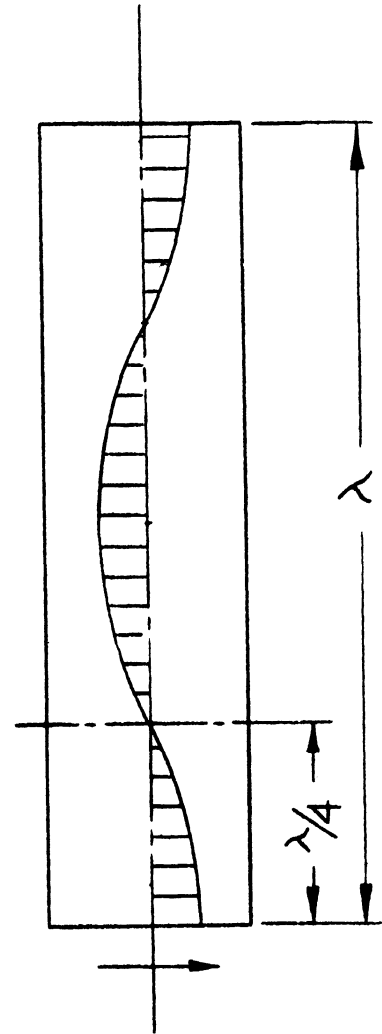


TABLE VIII
 FREQUENCIES OF SHEAR MODES*
 (kcs)

Bar Length, in.	Bar Length = $n\lambda/4$											
	n=1	n=2	n=3	n=4	n=5	n=6	n=7	n=8	n=9	n=10	n=11	n=12
2-1/2	12.2	24.4	36.6	48.8	61.0	73.2	85.4	97.6	109.8	122.0	--	--
5	6.1	12.2	18.3	24.4	30.5	36.6	42.7	38.8	54.9	61.0	67.1	73.2
10	--	6.1	1.15	12.2	15.25	18.3	21.3	24.4	27.4	30.5	33.6	36.6
11	--	5.55	8.3	11.1	13.85	16.65	19.4	22.2	24.9	27.75	30.5	33.4
11-1/2	--	5.3	8.05	10.6	13.25	15.9	18.5	21.2	23.8	26.5	29.3	31.8
12	--	5.07	7.6	10.15	12.7	15.22	17.7	20.3	22.8	25.37	28.0	30.5
12-5/8	--	4.83	7.25	9.65	12.1	14.48	16.9	19.3	21.7	24.13	26.5	29.0

*See diagram below; frequencies based on a velocity of 122,000 ips.



$$f = C/l \quad (3)$$

where

f = frequency in cycles per second
 C = velocity of sound in inches per second
 l = distance in inches the wave front must travel before reflections produce the phase changes of one cycle

$$C_l = \frac{E}{\rho} \quad (4)$$

where:

C_l = velocity of plane longitudinal waves in inches per second
 E, ρ = same as in Eq. (1)

$$C_s = C_e \frac{1}{2(1 + \sigma)} \quad (5)$$

where:

C_s = velocity of shear waves in inches per second
 σ = Poisson's ratio

Table VIII lists the frequencies of standing shear waves for bars of various lengths. They were calculated from Eq. (5) for several modes made up of integral increments of quarter wave lengths. It is necessary to consider odd as well as even integers because of the possibility that there is either a node or an antinode at the point of tool contact.

APPENDIX B

TABLES OF FREQUENCY DATA

TABLE IX

LENGTHS OF QUARTER-WAVES— $\lambda/4$ *
(in.)

Bar Length, in. ($l = n\lambda/4$)	Number of Quarter-Waves, n											
	1	2	3	4	5	6	7	8	9	10	11	12
2.5	1.25	1.25	.833	.625	.500	.416	.357	.312	.277	.25	--	--
5	2.5	1.67	1.67	1.25	1.00	.833	.715	.625	.555	.5	.465	.416
10	5	3.34	3.34	2.5	2.00	1.67	1.43	1.25	1.11	1.0	.91	.833
11	5.5	3.67	3.67	2.75	2.2	1.83	1.57	1.38	1.22	1.1	1.0	.915
11.5	5.75	3.82	3.82	2.87	2.3	1.92	1.64	1.44	1.28	1.15	1.04	.96
12	6	4	4	3	2.4	2	1.71	1.5	1.33	1.2	1.09	1.0
12-5/8	6.32	4.2	4.2	3.16	2.63	2.11	1.80	1.58	1.4	1.26	1.15	1.05

*For the conditions represented in Table V.

TABLE X

FREQUENCIES OF CHIP SEGMENTS FOR ALL METALS*

(kcs)

Feed, ipt	Speed, fpm	Frequency	No. of Tests	Total Scatter, %
.010	1575	12.7	12	31
.008	1575	13.1	6	12
.008	1575	17.8	3	9
.004	1575	24.5	2	13
.008	3150	23.6	1	0
.010	3150	37.4	5	10
.008	3150	37.5	5	5
.008	1575	36.5	2	10
.004	1575	35.9	4	14
.008	3150	37.3	3	4
.002	1575	38.0	4	13
.006	3150	37.8	3	5
.006	2300	37.8	3	4
.008	3150	50.0	4	0
.008	6300	50.4	1	0
.008	1575	47.3	1	0
.002	1575	48.2	3	14
.008	6300	63.0	2	0
.010	6300	63.0	1	0
.006	6300	95.1	4	14
.002	3150	102.0	5	15
.002	3150	128.0	3	5
.002	1575	115.0	1	0
.002	6300	193.6	9	10

*Separated by cutting conditions.

TABLE XI

SUMMARY OF FREQUENCIES FOR ALUMINUM

Bar Length, in.	Overhang, in.	Feed, ipt	Speed, fpm	Frequency, cps	Length of Cut	
					in.	usec
11-7/8	1/2	.010	1575	12,600	.200	634
11-7/8	1/2	.010	1575	11,700	1.000	3170
12.64	1/2	.010	1575	13,200	1.000	3170
11-7/8	1/2	.010	3150	34,600	.200	317
11-7/8	1/2	.010	3150	34,000	1.000	1585
11-7/8	1/2	.010	3150	34,600	.200	317
12-5/8	1/2	.010	3150	27,700	1.000	1585
12-5/8	1/2	.010	3150	29,600	1.000	1585
10	1/2	.008	3150	50,000*	.200	317
10	1/2	.008	3150	38,000	.200	317
1 x 5	1-1/2	.008	3150	37,800	.200	317
1/2 x 5	1/2	.008	3150	50,000*	.200	317
1 x 2-1/2	1/2	.008	3150	31,500*	.200	317
10	1/2	.008	6300	56,500	.200	158
5	1/2	.008	6300	63,000	.200	158
5	1-1/2	.008	6300	63,000	.200	158
10	1-1/2	.008	6300	81,500*	.200	158
12-1/2	1/2	.004	1575	30,800	1.000	3170
12-1/2	1/2	.004	1575	30,500	1.000	3170
12-1/2	1/2	.004	3150	90,500	1.000	1585
12-1/2	1/2	.004	3150	88,000	1.000	1585
12-1/2	1/2	.004	3150	90,000	1.000	1585
12	1/2	.002	1575	44,800	1.000	3170
12	1/2	.002	1575	43,800	1.000	3170
12	1/2	.002	3150	90,800	1.000	1585
12	1/2	.002	3150	90,000	1.000	1585
12	1/2	.002	3150	88,200	1.000	1585
2-1/2	1/2	.002	3150	94,000	.200	317
5	1/2	.002	6300	195,000	.200	158
5	1-1/2	.002	6300	178,000	.200	158
2-1/2	1/2	.002	6300	183,000	.200	158
5	1/2	.002	6300	198,000	.200	158
2-1/2	1/2	.008	1575	14,150	.200	634
2-1/2	1/2	.002	1575	47,000	.200	634
5	1/2	.008	3150	31,500	.200	317
2-1/2	1/2	.008	6300	50,400	.200	158
11-1/8	1/2	.010	6300	63,000**	.200	158
12	1/2	.002	1575	33,000	1.000	3170
12.4	1/2	.010	1575	13,545	1.000	3170

*Mixed

**Mixed slightly

TABLE XII

SUMMARY OF FREQUENCIES FOR STEEL

Bar Length, in.	Overhang, in.	Feed, ipt	Speed, fpm	Frequency, cps	Length of Cut		Type of Steel
					in.	μsec	
11-1/2	1/2	.010	1575	9,800	1.000	3170	1090
10	1/2	.008	1575	12,600	.200	634	1018
2-1/2	1/2	.008	1575	12,600	.200	634	1018
2-1/2	1/2	.008	1575	14,800*	.200	634	1018
10	1/2	.008	1575	18,900*	.200	634	1042
10	1-1/2	.008	1575	17,300*	.200	634	1042
2-1/2	1/2	.008	1575	17,300*	.200	634	1042
2-1/2	1/2	.008	3150	37,800**	.200	317	1018
10	1/2	.008	3150	(continuous)	.200	317	1018
10	1/2	.008	3150	37,800	.200	317	1042
10	1-1/2	.008	3150	50,000	.200	317	1042
10	1/2	.008	3150	50,000	.200	317	1042
2-1/2	1/2	.0037	1575	23,000	1.000	3170	1090
11-1/2	1/2	.0035	1575	26,100	1.000	3170	1090
11-1/2	1/2	.0035	3150	75,600*	1.000	3170	1090
10	1/2	.002	1575	34,600	.200	634	1018
2-1/2	1/2	.002	1575	44,000*	.200	634	1042
11-1/2	1/2	.002	1575	38,400*	1.000	3170	1090
11-1/2	1/2	.002	1575	34,600	1.000	3170	1090
10	1/2	.002	3150	94,000	.200	317	1042
2-1/2	1/2	.002	3150	126,000	.200	317	1042
11-1/8	1/2	.010	1575	9,800	1.000	3170	1090
11-1/8	1/2	.010	1575	10,000	1.000	3170	1090
11-1/8	1/2	.010	1575	11,200	1.000	3170	1090
11-1/8	1/2	.010	1575	11,200	1.000	3170	1090
11-1/8	1/2	.010	1575	12,600	1.000	3170	1090
11-1/8	1/2	.004	1575	29,400	1.000	3170	1090
11-1/8	1/2	.004	1575	30,400	1.000	3170	1090
10	1-1/2	.008	1575	14,200	.200	634	1018
10	1-1/2	.002	3150	126,000	.200	317	1018
11-1/16	1/2	.010	1575	11,400	1.000	3170	1090
11-1/16	1/2	.010	1575	10,400	1.000	3170	1090

*Mixed

**Very weak

TABLE XIII

SUMMARY OF FREQUENCIES FOR B120-TITANIUM

Bar Length, in.	Overhang, in.	Feed, ipt	Speed, fpm	Frequency, cps	Length of Cut	
					in.	μ sec
10	1/2	.008	3150	23,600	.200	317
10	1/2	.008	3150	36,200	.200	317
10	1-1/2	.008	1575	34,700	.200	634
10	1/2	.008	1575	47,300	.200	634
2	1/2	.008	1575	38,400	.200	634
10	1/2	.002	1575	115,000	.200	634
10	1/2	002	3150	132,000	.200	317
12-1/2	1/2	005	1575	115,000	1.000	3170

APPENDIX C

ANALYSIS OF IMPACT CONDITIONS

The following analysis applies to a freely falling sphere and the effects of its impact upon the end of a vertical metal bar. In this case, a 1/4-in. steel ball is dropped 9 in. onto the end of a cylindrical steel bar. The equations for the deflection of the sphere upon impact and the maximum pressure are those of Timoshenko.

The velocity, v , of the sphere upon impact is:

$$(1) \quad v = \sqrt{2gh}$$

where $g = 386 \text{ in./sec}^2$
 $h = 9 \text{ in.}$
 $= 84.2 \text{ in./sec}$

$$\therefore \text{Impact velocity} = 0.0000842 \text{ in./}\mu\text{sec}$$

The deflection, α , of the sphere upon impact is:

$$(2) \quad \alpha = 1.23 \left(\frac{P}{E} \right)^{2/3} \frac{1}{R^{1/3}}$$

where $R =$ radius of sphere, $1/8 \text{ in.}$
 $E =$ modulus of elasticity of steel 30×10^6
 $P =$ impact load in pounds

$$\therefore \alpha = 1.23 \frac{P}{30 \times 10^6} \frac{1}{(1/8)^{1/3}}$$

$$(3) \quad \therefore \text{Impact load in pounds, } P = 7.78 \times 10^6 \alpha^{1.5}$$

The total work done on the sphere as a result of deflection (α under an impact load of $P \text{ lb}$ is:

$$(4) \quad \text{Work done} = \int_0^{\alpha} Pd\alpha$$

Substituting for P ,

$$\text{Work done} = \int_0^{\alpha} 7.78 \times 10^6 \alpha^{1.5} d\alpha$$

$$\text{Integrating work} = 3.11 \times 10^6 \alpha^{2.5} \text{ in-lb}$$

Therefore the work done without loss is equivalent to the potential energy of the sphere prior to its fall.

$$(5) \quad \text{Potential energy of the sphere} = \frac{W}{h}$$

where W = weight in pounds
 h = height in inches

$$W = \frac{4}{3}\pi \frac{1}{8}^3 \times .28$$

$$= 0.00225 \text{ lb}$$

$$\therefore \text{Potential energy} = 0.02 \text{ in-lb}$$

(6) Work done = potential energy

$$3.11 \times 10^6 \alpha^{2.5} = 0.02$$

$$\therefore \alpha = 5.3 \times 10^{-4} \text{ in.}$$

(7) Using this value in the equation (3) for impact load, P = 95 lb

(8) Maximum pressure from impact, $q_0 = .388 \left[\frac{PE^2}{R^2} \right]^{1/3}$

$$\therefore q_0 = 682,000 \text{ psi}$$

Therefore the impact is inelastic.

If the impact were elastic, the contact time for the deflection, α , for the sphere as it impacts at 84.2 in./sec would be:

(9) Impact time = $\frac{\alpha}{v}$

$$\therefore \text{Impact time} = 25 \text{ } \mu\text{sec}$$

(10) Similar quantitative information can be obtained for other metals by substitution of the corresponding values for modulus of elasticity and Poisson's ratio into the general equations of Ref. 2.

REFERENCES

1. Air Material Command Technical Report No. 60-7 635, "Ultra High Speed Machining," Lockheed Aircraft Corp., 1960.
2. S. Timoshenko, "Theory of Elasticity," McGraw-Hill, New York, 1934, pp. 339-352.

UNIVERSITY OF MICHIGAN



3 9015 02841 2099